IEEE Access
Multidisciplinary | Rapid Review | Open Access Journal

Received July 8, 2021, accepted July 28, 2021, date of publication July 30, 2021, date of current version August 9, 2021.

Digital Object Identifier 10.1109/ACCESS.2021.3101690

Wireless Characterization and Assessment of an UWB-Based System in Industrial Environments

IMANOL PICALLO GUEMBE[1], PEIO LOPEZ-ITURRI[1,2], HICHAM KLAINA[3], GUILLERMO GLARIA EZKER[4], FÉLIX SÁEZ DE JAUREGUI URDANOZ[4], JOSÉ LUIS ZABALZA CESTAU[4], LEYRE AZPILICUETA[5], (Senior Member, IEEE), AND FRANCISCO FALCONE[1,2], (Senior Member, IEEE)

[1]Electric, Electronic and Communication Engineering Department, Public University of Navarre, 31006 Pamplona, Spain
[2]Institute of Smart Cities, Public University of Navarre, 31006 Pamplona, Spain
[3]Department of Teoría de la Señal y Comunicación, University of Vigo, 36310 Vigo, Spain
[4]NAITEC—Technological Center for Automotive and Mechatronics, 31006 Pamplona, Spain
[5]School of Engineering and Sciences, Tecnologico de Monterrey, Monterrey 64849, Mexico

Corresponding author: Francisco Falcone (francisco.falcone@unavarra.es)

This work was supported in part by the European Union's Horizon 2020 Research and Innovation Programme (Stardust-Holistic and Integrated Urban Model for Smart Cities) under Grant 774094, in part by the Ministerio de Ciencia through the Innovación y Universidades, Gobierno de España (Agencia Estatal de Investigación, Fondo Europeo de Desarrollo Regional—FEDER, European Union) under Grant RTI2018-095499-B-C31 IoTrain, and in part by the Gobierno de Navarra-Departamento de Desarrollo Económico under Grant 0011-1365-2019-000097 OEE LOG.

ABSTRACT The advent of Indsutrial Internet of Things is one of the main drivers for the implementation of Industry 4.0 scenarios and applications, in which wireless communication systems play a key role in terms of flexibility, mobility and deployment capabilities. However, the integration of wireless communication systems poses challenges, owing to variable path loss conditions and interference impact. In this work, an Ultra-Wideband (UWB) system for indoor location in very large, complex industrial scenarios is presented. Precise wireless channel characterization for the complete volume of a logistical plant is performed, based on 3D hybrid ray launching approximation, in order to aid network node design process. Wireless characterization, implementation and measurement results are obtained for both 4 GHz and 6 GHz frequency bands, considering different densities of scatterers within the scenario under test. Time domain estimation results have been obtained and compared with time of flight measurement results, showing good agreement. The proposed methodology enables to perform system design and performance tasks, analyzing the impact of variable object density conditions in wireless channel response, providing accurate time of flight estimations without the need of complex channel sounder systems, aiding in optimal system planning and implementation.

INDEX TERMS Industrial Internet of Things, industry 4.0, ultra-wideband, 3D ray launching, wireless sensor networks, wireless channel characterization.

I. INTRODUCTION

Industry digitalization to a large degree is supported on Industry 4.0, which will enable companies to combine advanced techniques in the fabrication and operation process together with smart technologies, thanks mainly to the Industrial Internet of Things (IIoT) [1]. The IIoT takes advantage of the features that IoT (Internet of Things) offers in industrial scenarios thanks to information gathering necessary for the process automation using specific sensors and devices, for example, wireless sensor networks (WSN). In environments such as factories and industrial plants, an increase in productivity is sought through predictive and remote maintenance to monitor manufacturing equipment, as well as the implementation of smart logistics for asset monitoring and load control. In this way, the IIoT is able to increase productivity levels efficiently by optimizing resources.

The use of WSNs in industrial environments is steadily increasing. An overview of the latest emerging IIoT solutions is presented in [2], focusing on the challenges

The associate editor coordinating the review of this manuscript and approving it for publication was Ivan Wang-Hei Ho.

associated with efficiency, availability, performance, interoperability, reliability and security in industry. In fact, in order to obtain the above-mentioned IIoT benefits, a dense deployment of devices is needed, leading to an energy efficiency problem and significant wireless channel interference. These constraints requires specific wireless channel and coverage/capacity analysis prior to system deployment. In this sense, in [3], a novel design methodology is presented to get trade-off and better performance among the three main requirements of an IIoT wireless system: Power, latency and reliability. In [4], an example of IIoT application on data management in a large petrochemical plant is presented, showing industrial WSNs as a good solution to overcome industrial requirements.

Within WSNs, one of the technologies that, in recent years, is gaining popularity, especially in industrial environments, is UWB (Ultra-Wideband). This technology is based on the IEEE 802.15.4a and 802.15.4z standards, offering high positioning accuracy, in the range of centimeters, thanks to the transmission of shorter pulses in a wide frequency range from 3.1 GHz to 10.6 GHz. It offers advantages over other technologies such as Bluetooth, providing high-speed transmission (up to 27 Mbps) and low consumption. In [5], an overview of the IEEE 802.15.4a standard focusing on design considerations and specification of UWB systems (ranging estimation techniques) for sensor networks implementation is presented. The next references describe different UWB localization systems and their performance in different indoor environments. Reference [6] presents a development of an embedded UWB indoor localization system with high accurate and low latency using an optimized STM32L4 microcontroller and two-way ranging algorithm. Reference [7] proposes an UWB multi-channel anchor for indoor localization based on the technique of time difference of arrival evaluated in multipath and Non-Line of Sight (NLoS) conditions. In [8], UWB commercial systems (Ubisense, DecaWave, BeSpoon) in NLoS (Non-Line of Sight) conditions are evaluated, concluding that the DecaWave system presents the higher accuracy and best performance. Reference [9] presents the UWB propagation modelling and characterization in a large indoor scenario where the obtaining results can be used for sensor network deployment. In [10], the comparison and evaluation of the performance of UWB and BLE (Bluetooth low Energy) commercial systems for indoor localization in different industrial environments are analyzed. Reference [11] presents a software location and tracking of forklift trucks using UWB technology in an industrial environment providing an acceptable accuracy in LoS (Line of Sight) conditions between tag and anchors. In [12], a combination of localization systems using UWB and Pedestrian Dead Reckoning (PDR) based methods are analyzed in order to provide a strong and reliable tracking of workers in factory environments. Reference [13] evaluates an UWB system in a dense node network providing improved mathematical models that ensure to know the supported user density of the localization system. In [14] an analysis of the UWB channel for ranging purposes using a Ray Tracing tool that validates in terms of path loss and small-scale fading is presented. Reference [15] describes an experimental assessment of the impact of the body wearable sensor on the UWB system and performing an error model regarding the shadowing effect. Reference [16] presents an UWB positioning system for reducing the human body shadowing for wearable sensors at a sub-meter level of localization accuracy.

The use of UWB technology in industrial environments, such as factories or logistics plants, enables a real-time localization of the load, forklifts or workers, resulting in an increase of productivity. Since industrial environments are high-reflective scenarios, owing to the presence of a large desnity of scatterers, with NLoS conditions given by obstacle presence and relevant electromagnetic interference, it is necessary to carry out radio characterization tasks before any devices deployment. In order to analyze the feasibility of UWB-based system deployment in an industrial environment, which is electromagnetically complex, this work provides an extensive wireless channel analysis in a real logistics plant with the aim of providing assessment in the use of UWB technology.

The UWB-based system under test has been deployed in the Truck & Wheel (T&W) Logistics plant, located in Arazuri, Navarre (Spain). The T&W Group offers innovative supply chain activities and logistics, agile solutions and reliable transportations for industries such as the automotive, manufacturing, mass market and textiles [17]. The logistics plant analyzed in this work is divided into three defined zones where the 2nd zone has been selected to deploy the UWB system due to the high load density, consisting of ten long racks of five pallets floors and separated by six corridors.

In order to carry out the radio characterization of the logistics plant, an extensive series of RF (Radio Frequency) measurements has been performed to validate the deterministic estimations provided by the 3D Ray Launching (3D-RL) algorithm, which are required for optimized deployment of the devices. Such coverage/capacity simulations consider the dimensions and the electrical properties of the objects within the plant. In addition, an analysis and comparison with several empirical propagation models, specifically with the IEEE 802.15.4a standard in industrial environments, are presented to highlight the deviation in relation with measurements compared with the 3D-RL approach, mainly given by the inherently volumetric estimations given by the later.

Once the radio channel characterization of the plant has been obtained, the deployment of UWB devices is presented and evaluated. For that purpose, different UWB-based kits are discussed, selecting the DecaWave MDEK1001 development kit due to its high accuracy and reliability [8]. As an initial approximation, coverage maps based on the 3D-RL simulations are shown, which provides the best deployment option according to received power levels. The main goal is to test UWB technology and its performance in a harsh RF logistics environment for indoor assets location and tracking applications. The assets that could be tracked within logistic

scenarios are vehicles (Forklifts and Automated Guided Vehicles), containers, pallets, tools, instrumentation or workers. According to the radio-planning task and other technical considerations, the deployment was carried out, and the acquired anchors' results are presented. In order to evaluate the UWB-based localization system, a comparison of the ToF (Time-of-Flight) data provided by DecaWave kits and estimations based on time-domain simulations using the 3D-RL tool are shown. The results obtained show that in 90% of T&W Logistics plant, the estimated localization accuracy is less than 30cm. The proposed system will ensure the logistics process's automation and control, reporting accurate real-time location of the load, tracking and loaded/unloaded confirmation, thanks to an optimized and low power UWB-based system deployment.

The main contributions of this work are the following:

- Specific simulation modules have been developed in order to dynamically generate objects in order to modify the density of the loading elements of the pallet, enabling the analysis of the impact of warehouse item distribution and density in wireless channel performance, consider all the morphological details within the scenario under analysis.
- Time domain analysis has been performed and tested with measurement results for UWB device deployment time of flight results, in a realistic location-based application showing good agreement and low average errors.
- The in house implemented 3D Ray Launching code can be employed as an analysis tool applicable for the design and deployment phases of UWB systems within complex indoor logistical scenarios, without the need of performing complex channel sounder based measurements.

This paper is organized as follows: Section II describes the wireless characterization of an industrial environment. Section III presents the measurement and results obtained from the T&W Logistics plant. Section IV is focused on UWB technology deployment and assessment. Conclusions of the results are presented in Section V.

II. INDUSTRIAL ENVIRONMENT CHARACTERIZATION

The advent of Industry 4.0 paradigms, taking advantage of IoT and Cyber Physical Systems, requires connectivity capabilities within industrial scenarios. Traditional field bus communications and workshop level connections are progressively combined with wireless communication systems, owing to flexibility, ease of deployment and scalability features, among others [18]. The use of wireless communication systems however is also subject to multiple issues, including impact in propagation losses owing to dense clutter, leading to shadowing given by non line of sight conditions and fast fading owing to multipath propagation. Moreover, industrial scenarios are potentially prone to relevant interference, given by external interference sources (e.g., power electronics switching sources, brush motors, high voltage welding devices, etc.), as well as by intra system or inter system sources. Moreover, concerns are also present in relation with security issues, given by potential intrusion attacks. These issues and the need to further enable the integration of wireless communication systems within industrial environments has lead to different studies in order to characterize and propose mitigation/adaptation techniques, which is particularly relevant in the case of IIoT applications [19]. In [20], the impact of variable delay, given by inherent indoor propagation conditions with high obstacle density and interference are described, applicable to OFDM based transmission within the 2.245 GHz and 5.4 GHz frequency bands. Propagation conditions for the case of line of sight, obstructed line of sight and non line of sight have been described with magnitude/phase measurements in the 2GHz to 6 GHz frequency range [21]. Raw data measurement sets have also been obtained in order to gain insight in wireless channel conditions in industrial environments, considering operational conditions such as the presence of robot arms [22] in the 2.4GHz frequency range. Propagation conditions for UWB systems within industrial scenarios have also been described, considering different clutter conditions (low density and high density), providing measurement based estimation of parameters such as the path loss exponent, maximum excess delay or root mean square delay spread, for distances up to 9 meters [23].

In this section, a deterministic based volumetric approach will be described in order to perform wireless channel characterization as well as subsequent system performance analysis, for the full volume of the scenario under test and considering to a full extent all the elements within these scenarios.

A. SIMULATION PROCEDURE

In industrial environments, electromagnetic signal phenomena such as reflection, diffraction and scattering from different structures such as walls, machinery, production lines, etc., may result in relevant multipath propagation. Reference [24] presents the path loss measurement-based results from different industrial environments, showing path-loss exponent values less than two in some cases, indicating the presence of strong multipath propagation in the channel induced by highly reflective surfaces. This fact makes the wireless channel in an industrial environment to behave much differently when compared when typical environments such as residential or office environments. Because of that, it is compulsory to perform wireless channel characterization prior to the deployment of a wireless communication system in this type of environments.

Measurement-based techniques prove to be accurate approaches to channel modeling given a specific environment. Nevertheless, these techniques can result costly both in economic and time terms [25]. In order to reduce these costs, geometry-based modeling approaches can be used achieving a good trade-off between accuracy and time. In this work, an in-house three-dimensional Ray Launching technique has been used to characterize the industrial channel environment. The algorithm is based on geometrical optics (GO) and the uniform theory of diffraction (UTD). First, the scenario under

test is modeled in 3D considering all the obstacles within the environment. Electromagnetic properties of all the obstacles within the environment are considered by means of the conductivity and relative permittivity of all the materials at the frequency under analysis. Then, rays are launched from the transmitter antenna with a predetermined 3D angular and spatial resolution. When a ray hits an obstacle, a reflected and refracted ray are created according to Snell's law, and when a ray hits and edge, a new family of diffracted rays are created according to the UTD coefficients. It is worth noting that owing to the geometric-stochastic nature of the proposed algorithm, it consider any potential type of link (i.e., LOS, NLOS or partial NLOS).

As previously stated, the algorithm in based in the GO approximation combined with UTD, in three-dimensional approach, supported by Fresnel equations to model transmitted and reflected waves. The geometry of the scenario as well as the material parameters in terms of dispersive conductivity and dielectric constant is implement in Matlab, considering a discretized mesh of cuboids within the simulation volume. For a given interface of two mediums 1, and 2, where equivalent ray interaction occurs, the reflection coefficient $R^{\parallel\perp}$ and the transmission coefficient $T^{\parallel\perp}$ for the parallel and perpendicular polarization are obtained for the volume of the scenario under analysis by the following expressions:

$$R^{\parallel} = \frac{E_r^{\parallel}}{E_i^{\parallel}} = \frac{\eta_1 cos\,(\psi_i) - \eta_2 cos\,(\psi_t)}{\eta_1 cos\,(\psi_i) + \eta_2 cos(\psi_t)} \tag{1}$$

$$T^{\parallel} = \frac{E_t^{\parallel}}{E_i^{\parallel}} = \frac{2\eta_2 cos\,(\psi_i)}{\eta_1 cos\,(\psi_i) + \eta_2 cos\,(\psi_t)} \tag{2}$$

$$R^{\perp} = \frac{E_r^{\perp}}{E_i^{\perp}} = \frac{\eta_2 cos\,(\psi_i) - \eta_1 cos\,(\psi_t)}{\eta_2 cos\,(\psi_i) + \eta_1 cos(\psi_t)} \tag{3}$$

$$T^{\perp} = \frac{E_t^{\perp}}{E_i^{\perp}} = \frac{2\eta_2 cos(\psi_i)}{\eta_2 cos\,(\psi_i) + \eta_1 cos(\psi_t)} \tag{4}$$

where $\eta_1 = 120\pi/\sqrt{\varepsilon}_{r1}$, $\eta_2 = 120\pi/\sqrt{\varepsilon}_{r2}$, ε_{r1} and ε_{r2} are the relative permittivity of the medium 1 and 2, and ψ_i, ψ_r and ψ_t are the incident, reflected and transmitted angles respectively. $T^{\parallel\perp}$ Diffraction is taken into account by considering wedge diffraction, where new diffracted rays are generated. In the case of finite conductivity bi-dimensional wedge conditions, the calculation of diffracted components is characterized by detecting the corresponding object edges and applying the following diffraction coefficients [26], [27] (5), as shown at the bottom of the page, where $n\pi$ is the wedge angle, F the line source model, L the distance parameter (variable as a function of the propagating wave), $a^{\pm}$ are diffraction angle dependent coefficient, $R_{0,n}$ the reflection coefficients as a function of the corresponding material layer interfaces, and Φ_2 and Φ_1 the angles to the observation points before and after the diffraction wedge. The resulting total E-field components (i.e., GO and UTD) are given by [28],

$$E_{\mathrm{GO}}^{\perp\parallel} = \sqrt{\frac{P_{\mathrm{rad}} D_{\mathrm{t}}(\theta_{\mathrm{t}}, \emptyset_{\mathrm{t}})\eta_0}{2\Pi}} \frac{e^{-\mathrm{j}\beta_0 r}}{\mathrm{r}} \mathrm{X}^{\perp\parallel} L^{\perp\parallel} \tag{6}$$

$$E_{\mathrm{UTD}}^{\perp\parallel} = e_0 \frac{e^{-\mathrm{j}ks_1}}{s_1} D^{\perp\parallel} \sqrt{\frac{s_1}{s_2(s_1+s_2)}} e^{-\mathrm{j}ks_2} \tag{7}$$

where $\beta_0 = 2\pi f_{\mathrm{c}}\sqrt{\varepsilon_0\mu_0}$, $\varepsilon_0 = 8.854{\cdot}10^{-12}$F/m, $\mu_0 = 4\pi{\cdot}10^{-7}$H/m and $\eta_0 = 120\pi$ ohms. P_{rad} is the radiated power of the transmitter antenna, whereas $D_{\mathrm{t}}(\theta_{\mathrm{t}}, \emptyset_{\mathrm{t}})$ is the directivity considering a spherical coordinate system at an elevation angle θ_{t} and an azimuth angle ϕ_{t}. Parameter e_0 is the free-space field strength, k is the propagation constant and s_1, s_2 are the distances from the source to the edge and from the edge to the receiver point, respectively. In order to decrease computational cost, hybrid simulation combining 3D RL with diffusion equation based on transport theory. In this way, excess loss given by edge diffraction is estimated by calculating obstacle density within 2D planes and hence estimating aforementioned losses following [29]:

$$L_{ex}^{T}(r_a) \sim \frac{10\sqrt{2}\sigma_g p_o \log e}{A_0} r_a - 5log\left(\frac{\pi p_0 \sigma_g r_a}{\sqrt{2}A_0}\right) \tag{8}$$

where p_0 is the obstacle density, $\mathrm{A_0}$ the average obstacle cross-sectional area, σ_{g} the geometrical cross section of the obstacles per unit length and $\mathrm{r_a}$ is Tx-Rx radial distance.

All the channel information is extracted from the 3D environment model. The last step of the simulation procedure is to process the information to obtain the required results, such as received power, path loss, power delay profile, etc. A detailed description of the 3D-RL simulation operation can be found in [28]. In addition, the different predetermined parameters have been set according to previous convergence analysis in different environments, which can be found in [28], [30]. For the considered simulations,

$$D^{\parallel\perp} = \frac{-e^{(-j\pi/4)}}{2n\sqrt{2\pi k}} \left\{ \begin{array}{l} cot\left(\frac{\pi + (\Phi_2 - \Phi_1)}{2n}\right) F\left(kLa^{+}(\Phi_2 - \Phi_1)\right) \\ + cot\left(\frac{\pi - (\Phi_2 - \Phi_1)}{2n}\right) F\left(kLa^{-}(\Phi_2 - \Phi_1)\right) \\ + R_0^{\parallel\perp} cot\left(\frac{\pi - (\Phi_2 + \Phi_1)}{2n}\right) F\left(kLa^{-}(\Phi_2 + \Phi_1)\right) \\ + R_n^{\parallel\perp} cot\left(\frac{\pi + (\Phi_2 + \Phi_1)}{2n}\right) F\left(kLa^{+}(\Phi_2 + \Phi_1)\right) \end{array} \right\} \tag{5}$$

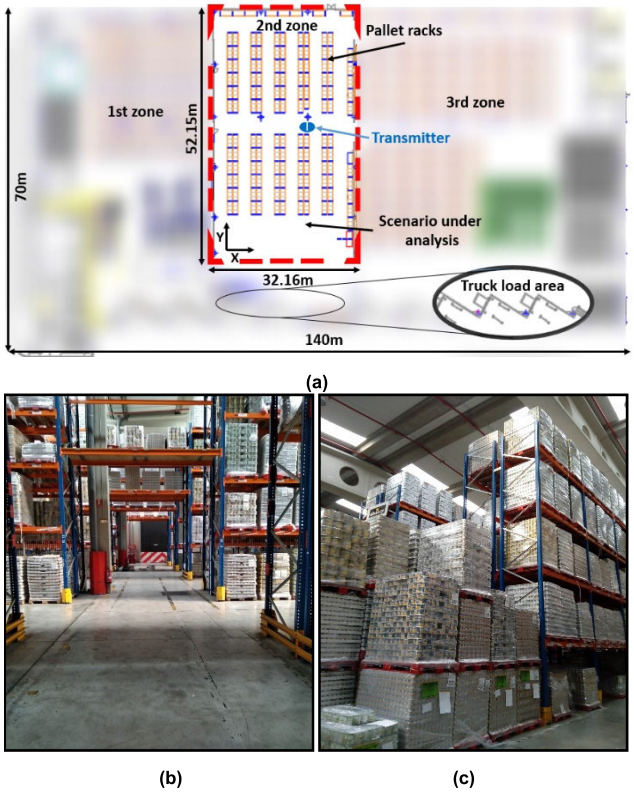

FIGURE 1. Truck & wheel logistics plant: (a) Plane of the three defined zones; (b) Distribution of bridges and racks; (c) Distribution of pallets in five floors racks.

the configured parameters will be shown in Table 2. The 3D-RL tool has been validated in the literature comparing the obtained results with measurement-based techniques, achieving accurate results with a root mean square error (RMSE) of 3-6 dB [14], [31], [32].

B. SCENARIO DESCRIPTION AND MEASUREMENTS SETUP

This subsection describes the industrial environment where both the radio-electrical characterization measurements and the deployment of the UWB devices have been carried out. In addition, the setup of measurements necessary to obtain results of the received power level at the frequencies of interest is presented. Since one of the goals in this work is the validation of these channel measurements, a realistic scenario has been implemented with the aid of the 3D-RL tool to obtain results close to reality, which are required for radio planning tasks.

The environment where RF measurements have been carried out is the T&W Logistics plant, located in Arazuri, Navarre (Spain). This plant is divided into three defined zones where the 2nd zone has been selected to deploy the UWB system (see Fig. 1a) due to the high load density (see Fig. 1b and 1c). This area is divided into ten long racks of five pallets floors and separated by six corridors. These racks are joined by two-floor bridges, as can be seen in Fig. 1b. There are also two more racks attached to the wall, as shown in Fig. 1a. The racks are made of metal beams, and the load

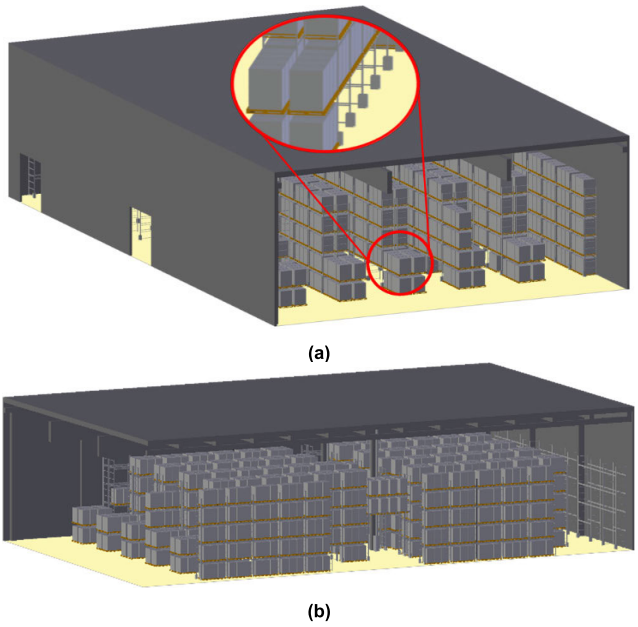

FIGURE 2. Truck & wheel logistics plant created with the 3D-RL tool.

TABLE 1. 3D-RL material properties.

Material	Conductivity (σ) [S/m]	Relative Permittivity (Ɛr)
Aluminum	$37.8 \cdot 10^6$	4.5
Wood	0.21	2.88
Glass	0.11	6.06
Concrete	0.02	25

of the pallets varies between glass and metal, depending on the stored product.

In Fig. 2, different views of the created 3D model of the analysis scenario with the 3D-RL tool are shown. This model has been generated to the maximum detail both in physical dimensions of the objects, as well as in the constitutive electrical properties of each material of these objects. In Fig. 2a, some gaps between the pallets are shown due to the fact that the scenario has been created with the same number of pallets as on the day the radio channel measurements were carried out. This is relevant since, as will be seen later, there are pallets between the transmitter and the receiver in the area where the measurements have been performed, which cause the channel variation from the LoS path to an obstructed channel (NLoS path). Table 1 shows the electrical properties of the materials used for the creation of the scenario, such as the conductivity and relative permittivity [33], [34].

Fig. 3 shows the setup of RF measurements performed at the 4 GHz and 6.2 GHz UWB frequency bands in T&W Logistics plant. The transmitter is located under a bridge at the height of 0.5m above the ground, as shown in Fig. 3a (real picture of the setup) or Fig. 3d (created scenario with the 3D-RL tool), using an adjustable tripod. In addition,

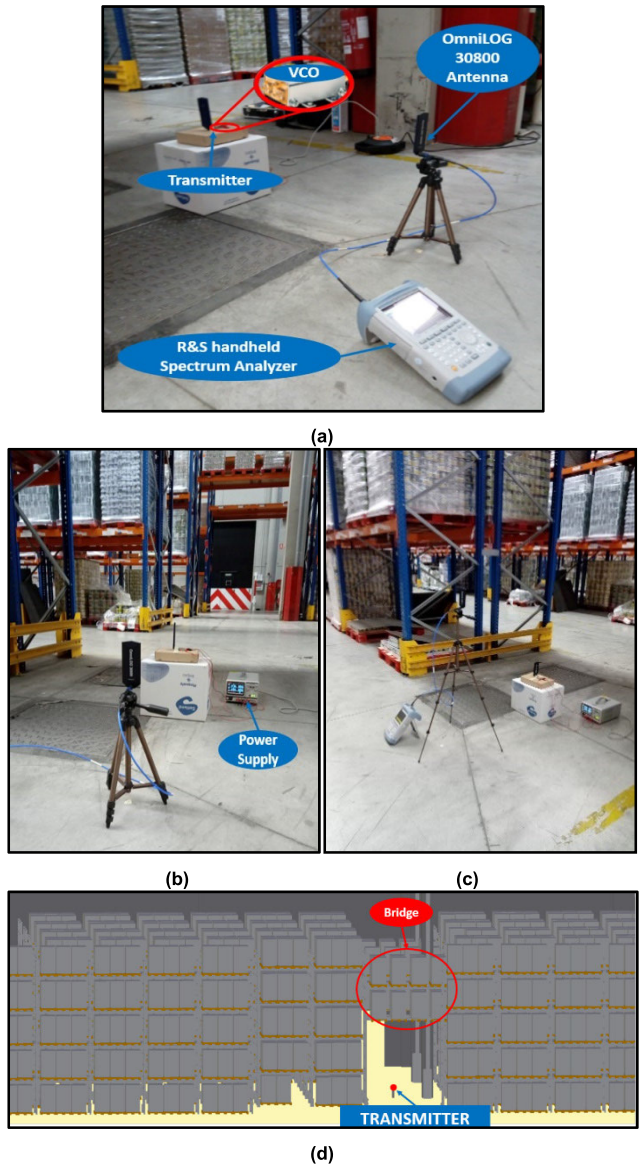

FIGURE 3. (a) View of the measurements setup; (b) Receiver antenna at the height of 0.5m; (c) Receiver antenna at the height of 1.5m; (d) View of the transmitter location under a full two-floor bridge using the 3D-RL tool.

the Agilent's FieldFox N9912A portable spectrum analyzer is also shown as a receiver to measure the received power level on the frequencies of interest. Measurements have been obtained at the heights of 0.5m and 1.5m to characterize the channel in the first two pallets floors.

A VCO (Voltage Controller Oscillator) device has been used as a transmitter to carry out the measurements. The ZX95-4000R model, which has 6.1 dBm transmission power for 4 GHz and the ZX95-6030C model, which has 2 dBm transmission power for 6.2 GHz have been used. The antennas employed in the measurements were DecaWave WB002 and OmniLOG 30800. The latter is an omnidirectional antenna, covering a wide frequency range from 300 MHz to 8 GHz with a variable gain depending on the frequency of operation. The corresponding setup (VCO and the OmniLOG 30800) is depicted in Fig. 3a. Table 2 shows the simulation parameters configured for the 4 GHz and 6.2 GHz frequencies, obtained according to previous convergence studies of the 3D-RL algorithm [28], [35].

TABLE 2. 3D-RL parameter configuration.

Parameter	Value	
Operation Frequency	4 GHz	6.2 GHz
Transmitted Power	6.096 dBm	2 dBm
Antenna Model/Gain	DecaWave WB002 / 2.2 dBi	OmniLOG 30800 / -8 dBi
Transmitter Height	0.43m	
Horizontal angular resolution ($\Delta\Phi$)	1°	
Vertical angular resolution ($\Delta\theta$)	1°	
Permitted maximum reflections	6	
Cuboids size (Mesh resolution)	50cm x 50cm x 50cm	
Diffraction phenomenon	Activated	

III. VALIDATION RESULTS

In this section, a set of simulation results will be presented for the 4 GHz and 6.2 GHz frequency bands. In order to validate these estimations, the results will be compared to the RF power level measurements and empirical models, such as the IEEE 802.15.4a in industrial environments previously mentioned. These simulation results will be analyzed when the plant is empty, (i.e. no pallets on the racks), and when the plant is full in terms of the number of pallets. These results are interesting to compare opposite cases in terms of load since the received power level in some areas could be low, close to the devices' sensitivity threshold, owing to multipath propagation.

Regarding the calculation of the IEEE 802.15.4a empirical model, reference [36] presents the IEEE document of the IEEE 802.15.4a channel modeling subgroup. This report describes the propagation models for UWB channels within the frequency range from 2 to 10 GHz and some environments, such as indoor office, outdoor and industrial, just to name a few. The frequency-dependence path is given by [36] as

$$PL\,(f) = 0.5 \cdot PL_o \cdot \eta_t \cdot \eta_r \frac{\left(f/f_c\right)^{-2\cdot(\kappa+1)}}{\left(d/d_o\right)^{n}} \tag{9}$$

where PL_o is the path loss at 1m distance, η is the efficiency of the antenna, f is the UWB bandwidth, κ is the frequency dependence of the path loss, n is the path loss exponent, d is the distance and d_o is the reference distance at 1m. The coefficient are based on measurements carried out in industrial environments in LoS and NLoS conditions [36], [37].

A. 4 GHz FREQUENCY BAND

Fig. 4a and 4b show 2D horizontal received power level distribution planes for 4 GHz, at the heights of 0.5m and 1.5m

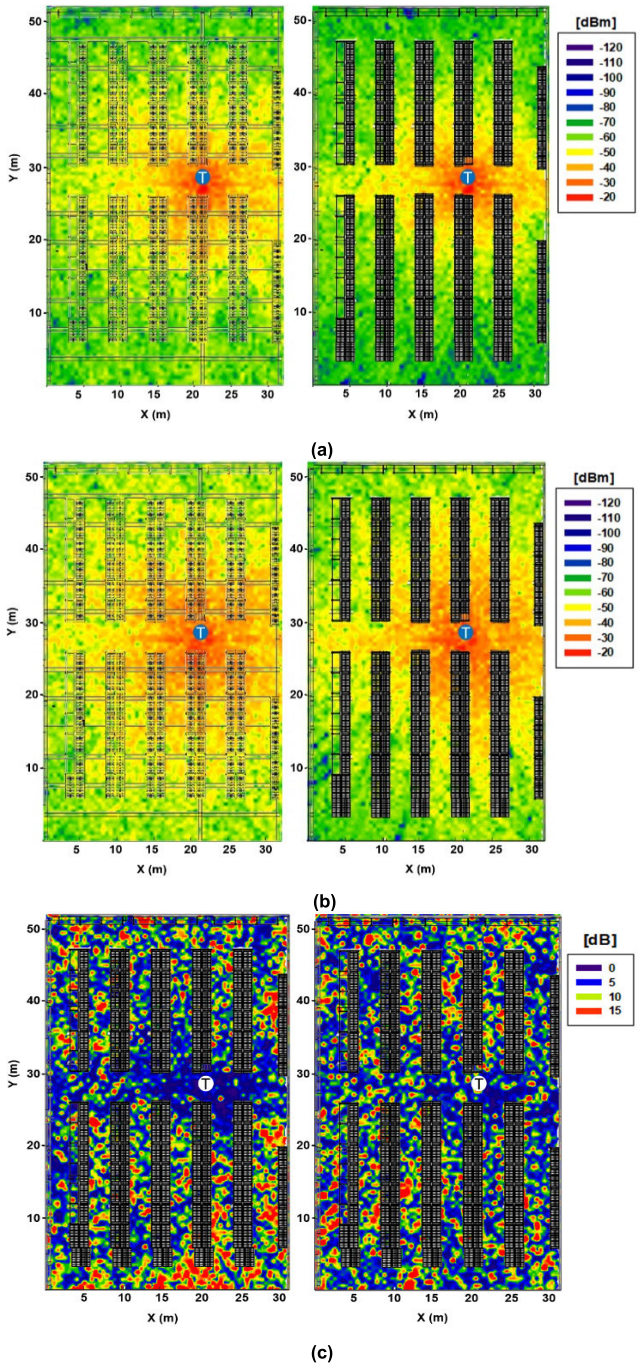

FIGURE 4. (a) Estimated 2D RF power distribution planes (XY) for 4 GHz at 0.5m height for empty and full plant; (b) Estimated 2D RF power distribution planes (XY) at 1.5m height for empty and full plant; (c) Difference in estimated power plane between full and empty plant for 0.5m and 1.5m height.

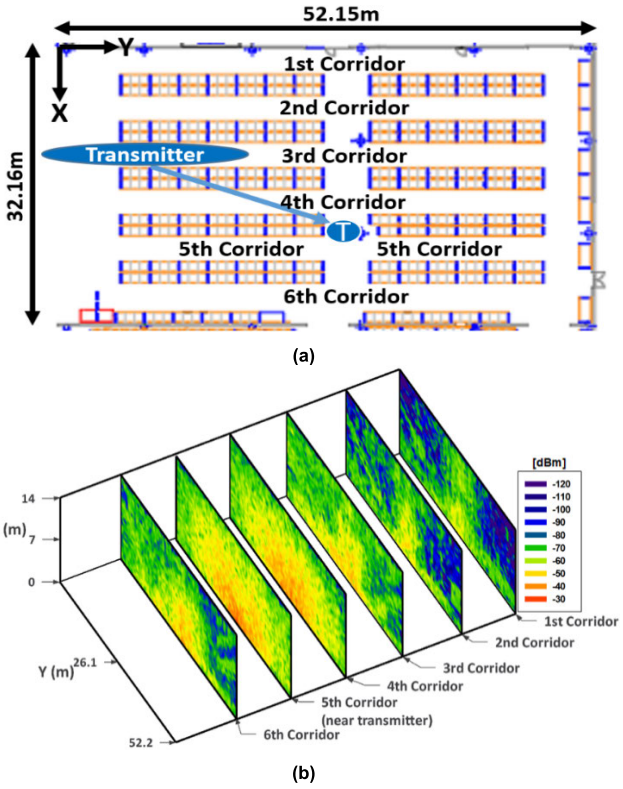

FIGURE 5. (a) Plane of T&W logistics plant; (b) Estimated RF power distribution bi-dimensional planes (YZ) corresponding to each corridor according to the load on the pallet racks during the measurements carried out.

for empty and full plant, using the RL tool. In addition, the racks' blueprint has been overlapped for detail of the power propagation within the plant. It must be taken into account that the bridges with pallets have not been represented in the blueprint because the bridges are at a higher height than that there is illustrated in those 2D cuts (see Fig. 3d). Simulation times span form 21000 seconds to 207000 seconds, as a function of scenario pallet loading conditions.

However, in the simulations, the bridges have been taken into account since they have a notable influence due to the fact that the transmitter is located just under one of these bridges. Note that some racks are depicted as empty in the case of the full plant results because they are not prepared to store pallets. For both figures, it is shown how a 100% increase in the number of pallets produces a visible increase in propagation losses as the distance increases, and the channel is obstructed with the different racks. Even with that, the received power level is optimal due to the transmission power and the low operating frequency. In order to highlight the variation in the received power level, Fig. 4c shows the RF power level difference between full and empty plant (of Fig. 4a and 4b). These planes represent positive increments in dB units, considering that 10-15 dB values are high variations. Therefore, the load increment causes variations in the wireless channel, which is relevant in device deployment planning.

As shown above, simulation results of horizontal planes of the scenario (XY-axes) have been presented, but as previously stated, the RL algorithm is three-dimensional, and so, in each simulation, results are obtained in the entire volume of the scenario. In this way, a complete radio characterization is achieved that will serve for radio planning tasks so that the best location of the nodes can be explored. In fact, in these industrial-type environments, it is relevant due to the different heights of the load. Therefore, Fig. 5b shows vertical power estimation planes (YZ-axes) for each corridor named

in Fig. 5a. As it can be seen, in the furthest corridors from the transmitter (corridor 1 and 2), the received power level decreases. There are high received power levels for the central area that connects all the corridors because of the LoS path until a certain height where the two-floor pallets bridges are located, which join the racks throughout the Y-axis.

The following figure presents the comparison of RF measurements with the simulation results provided by the 3D-RL tool. The amount of pallets on the simulated scenario follows the load on the pallet racks during the measurements carried out. As shown in Fig. 6a, measurements have been performed on four paths (A, B, C and D) at the heights of 0.5m and 1.5m. It is necessary to point out that it is measured each meter from the transmitter for paths A and B. However, for paths C and D, the first point is not at one meter from the transmitter because measurements are made in the center of corridor 5 every one meter, so there begin from path A. On path D, it is important to note that the last points from 22m, even there are no physical racks, between two and three pallet floors are stored as shown in Fig. 1c, and therefore, it has been indicated by adding graphic blocks to the racks in Fig. 6a. Regarding Fig. 6a, it can also be anticipated that paths A and B are LoS paths, but in paths C and D are LoS paths only at the first points (until 2-3m distance from path A) and then, they become NLoS or partial NLoS paths (gaps between the pallets cause increments in the received power level). The percentage of NLoS or partial NLoS points is about 55% in the case of the measurements for 4 GHz. Therefore, multipath propagation plays a key role in wireless radio characterization in this harsh environment.

In Fig. 6b, received power level results are presented for path A. It shows measurements, simulations provided by the 3D-RL and two previously analyzed empirical models (the Cost 231 multiwall and the IEEE 802.15.4a LoS and NLoS cases). As can be seen, the simulations results are well adapted to the variations of the wireless channel, providing accurate estimations with an average error of 2.3 dB and 1.35 dB at the height of 0.5m and 1.5m, respectively. Regarding the empirical models, the IEEE 802.15.4a model better fits in the LoS case because the path is unobstructed. The other models do not follow the trend of the received power level. In Fig. 6c, the obtained results for path B are presented. It shows how the received power level estimations of the 3D-RL tool for both heights are accurate, getting an average error of 1.51 dB and 1.21 dB, respectively. The IEEE 802.15.4a LoS empirical model follows the trend of measurements and simulations for both heights, whereas the Cost-231 multiwall model is not a good approximation for measurements.

In Fig. 6d and 6e, paths C and D, the first measurement point is under −40 dBm (unlike −35 dBm in paths A and B) because the first point is at a larger distance than one meter from the transmitter. In Fig. 6d, the results provided by the 3D-RL tool follow the variation of the results obtained in the measurements for both heights, that is, the power level

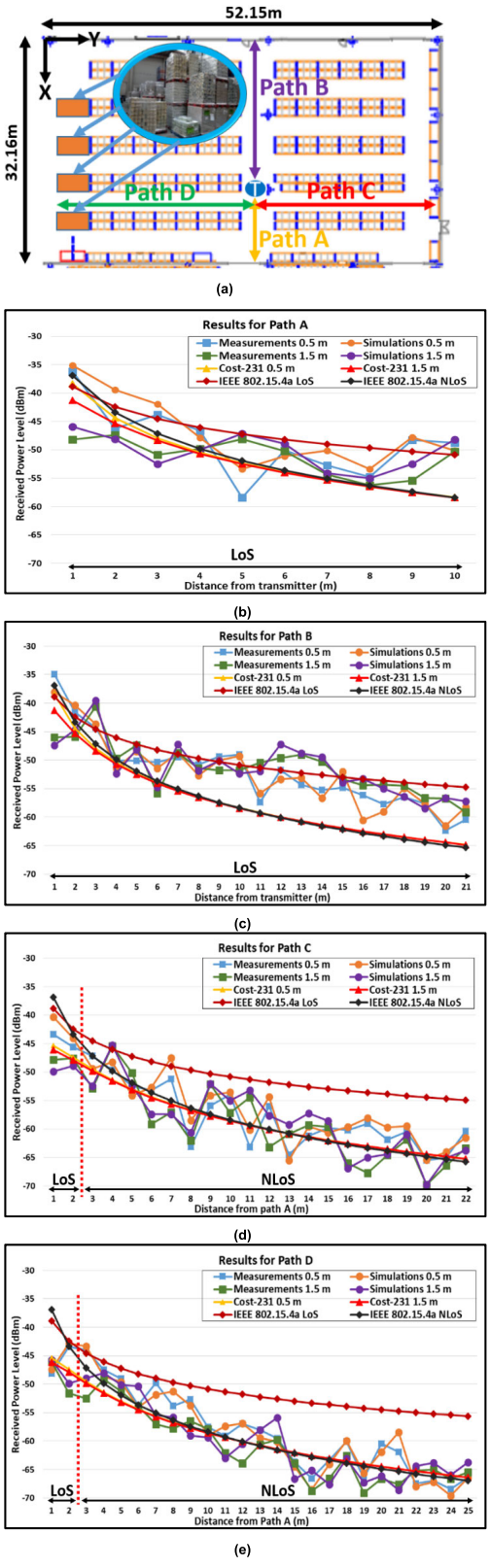

FIGURE 6. Comparison of the measurements, simulations using the 3D-RL tool and some empirical models (the Cost-231 multiwall and IEEE 802.15.4a) at the height of 0.5m and 1.5m for 4GHz: (a) Schematic view of the analyzed paths; (b) path A; (c) path B; (d) patch C; (e) path D.

TABLE 3. Root mean square error for 4 GHz.

RMSE	Path A	Path B	Path C	Path D
Simulations 0.5m	2.99	1.79	1.95	1.33
Simulation 1.5m	1.60	1.38	1.81	2.09
Cost-231 0.5m	5.26	5.56	2.94	3.15
Cost-231 1.5m	4.06	7.38	3.43	2.48
IEEE 802.15.4a LoS 0.5m	4.46	3.36	7.28	7.99
IEEE 802.15.4a LoS 1.5m	5.17	3.15	9.01	9.82
IEEE 802.15.4a NLoS 0.5m	5.18	5.60	3.21	3.48
IEEE 802.15.4a NLoS 1.5m	5.03	7.66	4.25	3.45

variations produced by the wireless channel. As expected, it is a path with a line of sight points and others with NLoS, and therefore, as shown in the graph, the empirical model that follows the trend of the measurements would be a combination of the IEEE 802.15.4a LoS and NLoS cases. The average error for path C is 1.63 dB and 1.35 dB, respectively. Finally, in Fig. 6e, path D results are shown, where the 3D-RL continues to provide accurate results concerning measurements. The average error is 1.06 dB and 1.8 dB. Furthermore, as in the previous case, combining the model for a line of sight and obstructed sight for industrial environments would give the best approximation to the results' trend. Table 3 presents the RMSE for 4 GHz, between measurements and deterministic (simulations) and empirical models to show the performance of each one of them. As can be seen, the simulation results with the 3D-RL show the lowest RMSE and, therefore, best approximates the multipath propagation. In the case of empirical models, the IEEE 802.15.4a for paths A and B, the RMSE is lower for LoS model, as they are paths with a full line of sight. In the case of paths C and D, the lowest RMSE occurs for the IEEE 802.15.4a NLoS due to the fact that from the third measurement point (see Fig. 6d and 6e), the sight is obstructed by the pallets on the racks.

B. 6.2 GHz FREQUENCY BAND

In this subsection, simulation results will be presented for the 6.2 GHz frequency using the RL tool. As in the case of 4 GHz, simulation results will be shown for opposite cases regarding the load within the plant. In addition, the measurements will be presented, comparing them with the simulations obtained by the 3D-RL tool and with empirical models, exhibiting a better fit with measurements in the deterministic case. Fig. 7a and 7b show 2D received power level distribution planes at the height of 0.5m and 1.2m for empty and full plant. Regarding the results shown, the increase in the frequency produces a very significant increase in losses. In addition, in this case, the transmitted power is 2 dBm that is 4 dB lower than the transmitted power by the VCO device used in the 4 GHz measurements. It should also be noted that the OmniLog 30800 antenna has low gain for this frequency due to the wide bandwidth in which it can operate. In Fig. 7c, the RF power level difference between full and empty plant are shown (of Fig. 7a and 7b).

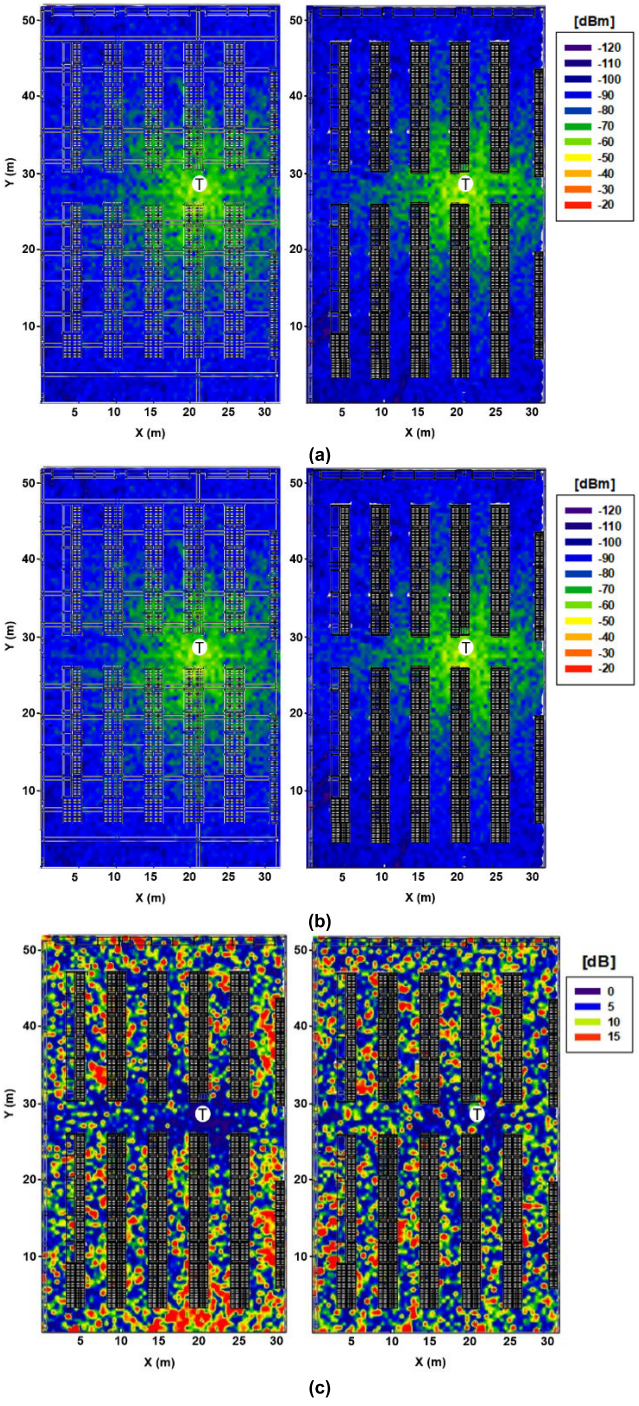

FIGURE 7. (a) Estimated 2D RF power distribution planes (XY) for 6.2GHz at 0.5m height for empty and full plant; (b) Estimated 2D RF power distribution planes (XY) at 1.2m height for empty and full plant; (c) Difference in estimated power plane between full and empty plant for 0.5m and 1.2m height.

In Fig. 8, the four paths (the same as in Fig. 6a) for the 6.2 GHz frequency are shown at the heights of 0.5m and 1.2m. For all paths, it can be seen the accuracy of the 3D-RL tool compared to the measurements carried out in the plant. For path A, the average error is 2.02 dB and 1.66 dB for both heights. In the case of path B, the average error

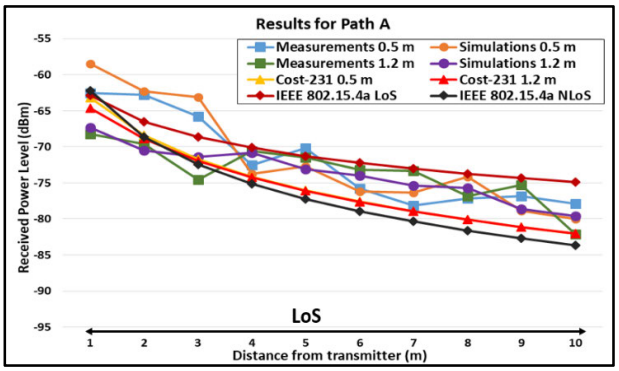

(a)

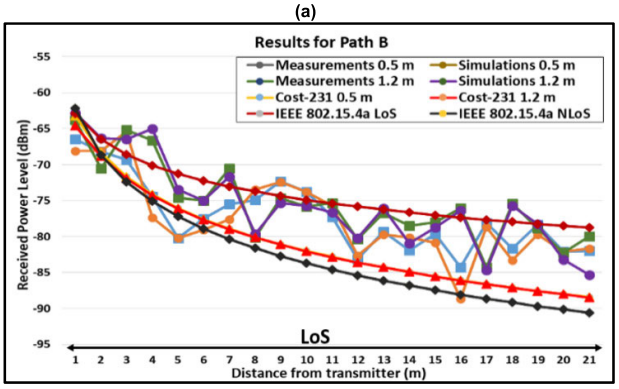

(b)

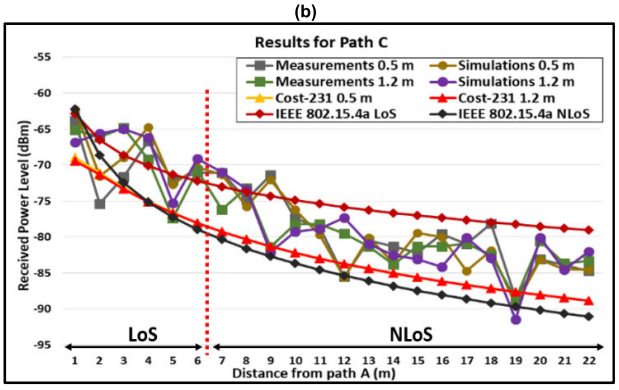

(c)

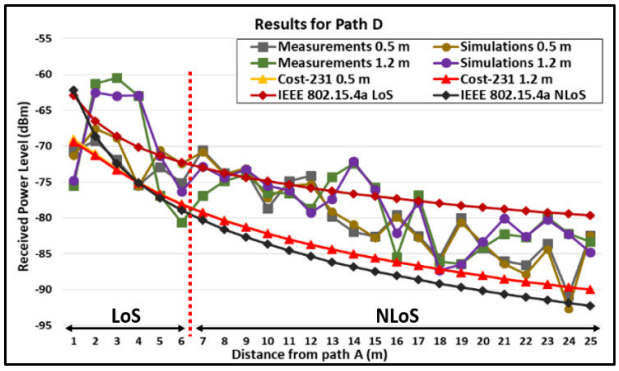

(d)

FIGURE 8. Comparison of the measurements, simulations using the 3D-RL tool and some empirical models (the Cost-231 multiwall and IEEE 802.15.4a) at the height of 0.5m and 1.2m for 6.2GHz: (a) path A; (b) path B; (c) patch C; (d) path D.

TABLE 4. Root mean square error for 6.2 GHz.

RMSE	Path A	Path B	Path C	Path D
Simulations 0.5m	2.29	1.79	1.84	1.22
Simulation 1.5m	1.95	1.76	1.85	2.07
Cost-231 0.5m	3.88	5.28	5.51	5.12
Cost-231 1.5m	3.90	6.61	4.83	7.43
IEEE 802.15.4a LoS 0.5m	3.06	4.02	4.57	4.90
IEEE 802.15.4a LoS 1.5m	3.69	3.08	4.42	5.41
IEEE 802.15.4a NLoS 0.5m	4.86	6.74	6.67	6.73
IEEE 802.15.4a NLoS 1.5m	5.07	8.11	5.76	8.83

between measurements and the 3D-RL tool is 1.31 dB and 1.18 dB for both heights. In paths A and B, the empirical model that best fits measurements is the IEEE 802.15.4a LoS, since both have a line of sight with the transmitter (as shown in Fig. 6a) at all the path. However, as mentioned above, it is an empirical model that follows a trend and does not consider the variations caused by multipath propagation.

In path C, the average error is 1.39 dB and 1.45 dB, and for path D, the average error is 0.92 dB and 1.44 dB for both heights, respectively. Both paths behave differently concerning line-of-sight path results. In fact, as in the 4 GHz results, they follow a trend that mixes empirical models in industrial environments of a line of sight (at the first measurement points) and vision obstructed by pallets (from 6-7m distance from path A). The percentage of NLoS or partial NLoS points is about 44% in the case of the measurements for 6.2 GHz. The Cost-231 multiwall, doesn't fit in any of the cases since it isn't based on measurements carried out in an industrial environment as the IEEE 802.15.4a model does. Table 4 presents the RMSE for 6.2 GHz between measurements and deterministic (simulations) and empirical models in order to show the performance of each one of them. As in the case of 4 GHz, the 3D-RL show the lowest RMSE. Regarding the IEEE 802.15.4a for paths C and D, the RMSE provides similar values for LoS and NLoS models due to the fact that the load in the T&W Logistics plant was lower during the 6.2 GHz measurements. Therefore, there are more gaps on the racks that cause a higher receiver power level (see Fig. 8c and 8d).

IV. UWB TECHNOLOGY DEPLOYMENT AND ASSESSMENT BY THE 3D-RL TOOL

Once the 3D-RL tool has been validated, the deployment of UWB devices is presented and evaluated. For that purpose, different UWB-based kits are discussed, selecting the DecaWave MDEK1001 development kit. In order to choose the best option for the devices' deployment, radio-planning tasks based on the 3D-RL simulations are presented. According to this, the deployment carried out in T&W Logistics plant is shown together with anchors' results during the system operation. Finally, a comparison of the ToF data provided by DecaWave kits and estimations based on time-domain

TABLE 5. DecaWave kits MDEK1001 vs EVK1000.

Parameter	MDEK1001 (DWM1001)	EVK1000
Radio Transceiver IC	DW1000 IEEE 802.15.4-2011 UWB	DW1000 IEEE 802.15.4-2011 UWB
Operation Frequency	6.240-6.739 GHz	3.5-6.5 GHz
Operation Channel	Channel 5 UWB	Channel 1,2,3 and 5 UWB
Bandwidth	500 MHz	500 MHz/channel
Preamble Length	128	Depends on channel
Data Rate	6.8 Mbps	6.8 Mbps
Transmitted Power	-17 dBm / 0 dBm	Programmable
Antenna Model/Gain	DecaWave WB003/ 2.5 dBi	External DecaWave WB002 / 2.2 and 3.3 dBi (4 and 6.5 GHz)
Sensitivity	-92/-98 dBm	-93 dBm
Ranging Accuracy	Within 10 cm	More than 10 cm
Additional Connectivity	Bluetooth Low Energy	No
Number of anchors	30 anchors per cluster	3 anchors per cluster
Ranging	Two-way ranging with 3-4 anchors	Two-way ranging with 2 anchors
Scalability	Yes	Limited
Packaging	Plastic enclosure for boards	No

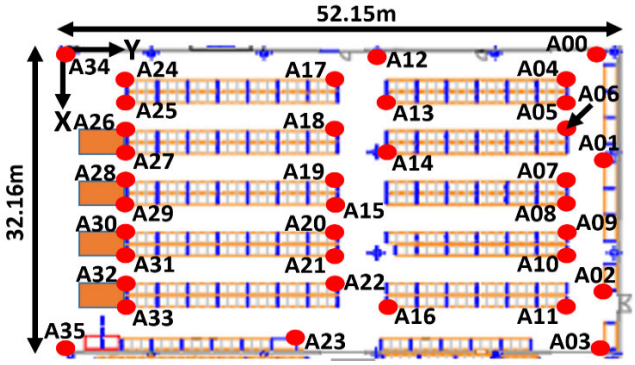

FIGURE 9. Illustration of a possible UWB anchors deployment covering all scenario within the plant to localize tags along the corridors.

simulations using the 3D-RL tool are presented to evaluate the UWB-based localization system.

A. UWB COMMERCIAL DEVICES

It has been reported that DecaWave technology behaves better under NLoS conditions than other options such as BeSpoon or Ubisense in terms of reliability and accuracy [8]. This is probably because DecaWave technology is the newest system providing the latest indoor localization techniques achieving centimeter range accuracy [38]–[40]. Among DecaWave technology options [41], two evaluation kits are available: MDEK1001 and EVK1000. Both kits are based on the radio transceiver IC DW1000 IEEE 802.15.4-2011 UWB. However, the EVK1000 kit is very limited and is not valid for a complex deployment, allowing a location test only with two reference anchors. The MDEK1001 kit is a complete tool that allows implementing an UWB infrastructure providing coverage in large areas

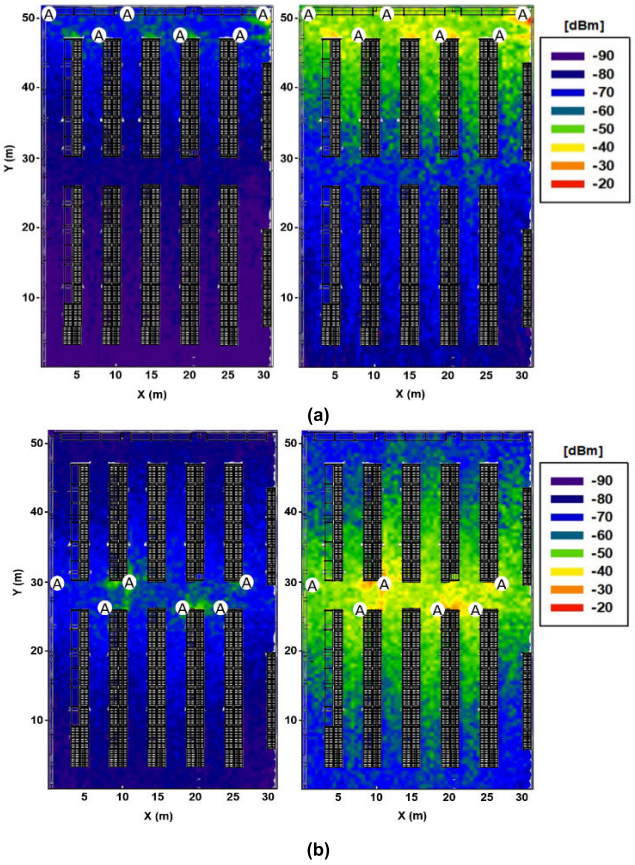

FIGURE 10. Estimated 2D RF power distribution planes (XY) for the full plant at the height of 1.5m when the transmitted power is −17 dBm (left) and 0 dBm (right), for the following anchors: (a) A00, A01, A03, A06, A09 and A11; (b) A12, A14, A16, A18, A20 and A22.

by installing up to 30 anchors and multiple labels with a position update frequency up to 10 Hz. It also includes all the necessary software, such as the stack called DecaWave Positioning and Networking Stack (PANS), firmware for Gateways on Raspberry Pi, MQTT protocol and, installation and monitoring applications by Web Server.

The comparison of the main characteristics of both kits are shown in Table 5. According to these properties, the MDEK1001 kit has been selected for UWB-based system deployment. As can be seen, the MDEK1001 kit works on UWB channel 5, so the UWB-based system radio planning and deployment have been carried out for the 6 GHz frequency band. It's worth noting that the procedure and radio planning tasks presented in the following section could be easily applied to other devices, including 4 GHz band-based solutions due to the versatility of the employed 3D-RL tool.

B. UWB-BASED SYSTEM DEPLOYMENT

In this subsection, UWB-based system deployment is presented together with the results provided by the anchors. As an initial approximation, a possible UWB anchors deployment is shown in Fig. 9 in order to cover all the logistics plant and localize the tags along the corridors. For this, DecaWave's recommendations for the deployment have taken

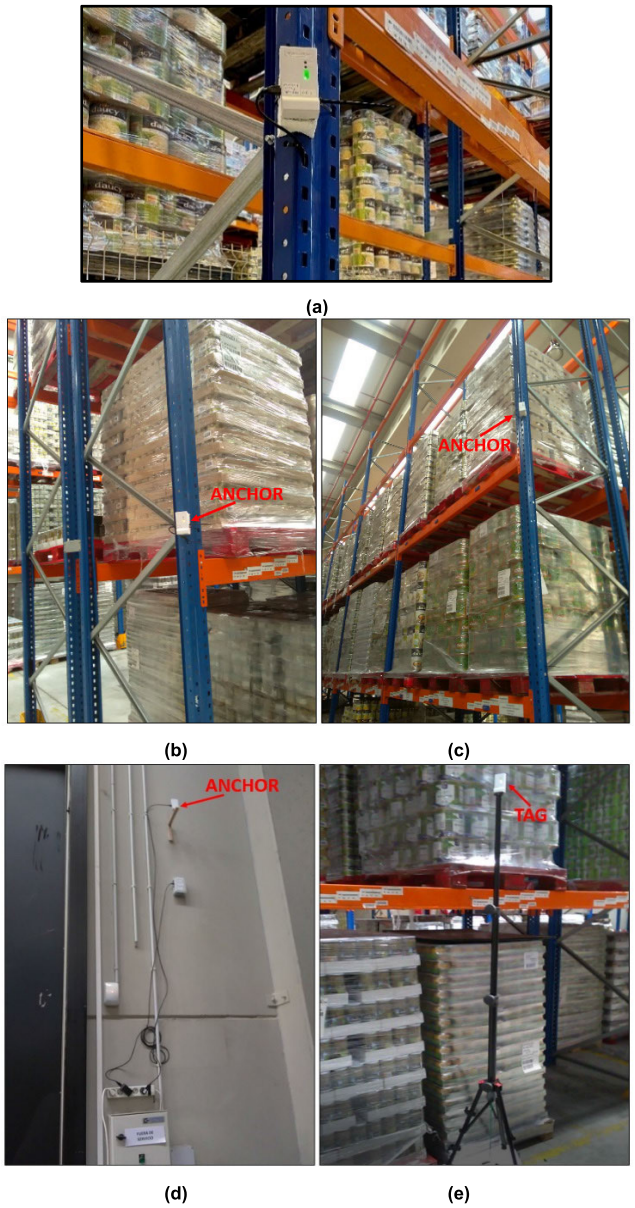

FIGURE 11. (a) Anchor's position on the rack; (b) and (c) Anchors' positions at the heights of 2m and 3m; (d) Anchor A12 on the wall (see Fig. 9); (e) Localizable tag along the corridor at the height of 2.4m.

into account. Firstly, it is not recommended to have more than 15-20m distance between the anchors, so the range is limited. In order to achieve high accuracy, it is recommended that the tag will be in LoS conditions with four anchors most of the time. The PANS stack algorithm determines four anchors to perform the trilateration based on the coordinates where they are located. One of the characteristics of UWB technology is that performance is maintained under NLoS conditions. However, in harsh environments in terms of RF propagation, such as the logistics plant analyzed in this work, the multipath propagation and signal attenuation have an important influence on degrading the localization operation, as shown in the validation results section. Thus, the deployment with a high density of anchors, illustrated in Fig. 9, ensures that the tag is in LoS conditions with the anchors.

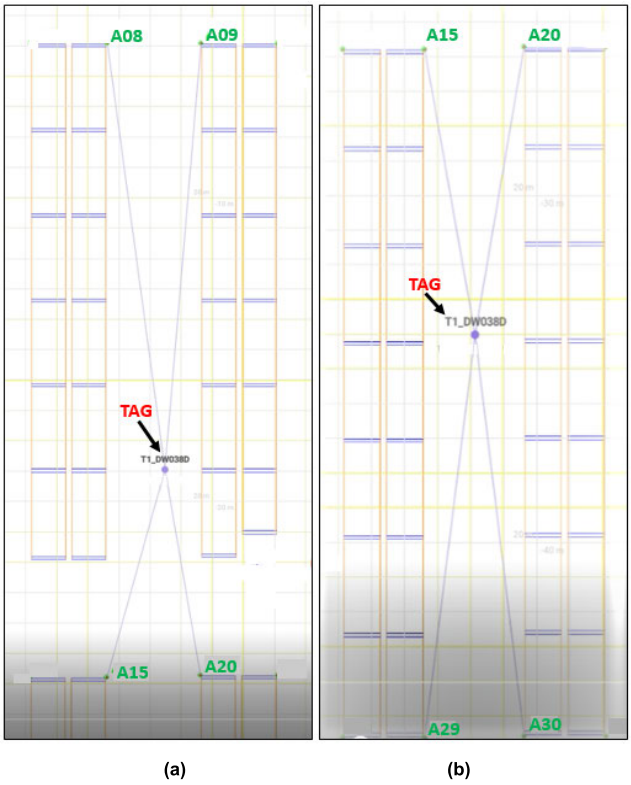

FIGURE 12. Capture of a real-time video of the tag tracking along corridor 4: (a) Test point 1: Using anchors A08, A09, A15 and A20; (b) Test point 2: Using anchors A15, A20, A29 and A30.

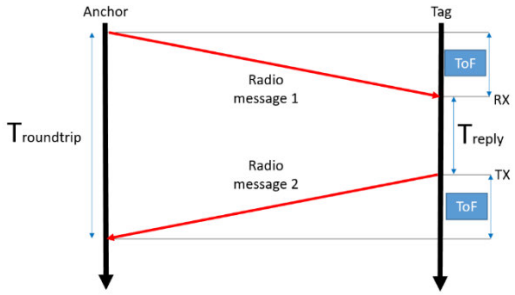

FIGURE 13. Two-ray ranging concept applied by DecaWave's devices.

FIGURE 14. An example of the data gathered for test point 1, where the distance between the tag 038D and anchors A08 (840B), A09 (CC84), A15 (88B4) and A20 (901B) is shown.

In order to optimize the deployment of the anchors and due to the limitation of 30 anchors per cluster (see Table 5),

TABLE 6. ToF and distance comparison between tag and anchors for DecaWave devices and 3D-RL tool for test point 1.

Tag ID	Anchor	DW ToF (ns)	3D-RL ToF (ns)	DW dist. (m)	3D-RL dist. (m)	Abs. Error (cm)
038D	A08	46.99	43.38	14.09	13.01	108
038D	A09	46.97	44.79	14.09	13.43	66
038D	A15	23.32	24.06	6.99	7.21	22
038D	A20	23.23	23.5	6.97	7.05	8

TABLE 7. ToF and distance comparison between tag and anchors for DecaWave devices and 3D-RL tool for test point 2.

Tag ID	Anchor	DW ToF (ns)	3D-RL ToF (ns)	DW dist. (m)	3D-RL dist. (m)	Abs. Error (cm)
038D	A20	27.95	24.04	8.38	7.21	117
038D	A15	28.09	27.08	8.42	8.12	30
038D	A29	38.98	40.13	11.69	12.04	35
038D	A30	38.96	39.0	11.69	11.70	1

radio-planning tasks have been carried out using the 3D-RL tool to get a reliable approximation of the number of nodes to distribute within the plant. For this purpose, several examples of simulations have been launched according to the parameters of Table 5, where the results of some of the anchors from A00 to A11 are shown in Fig. 10a and anchors from A12 to A22 are shown in Fig. 10b. Regarding transmission power, the certification document of the MDEK1001 kit set it in 0 dBm. However, the datasheet of the DWM1001 provides −17 dBm, so both cases have been considered. In this way, in Fig. 10, 2D horizontal coverage planes are presented for the full plant (worst case) at the height of 1.5m, when the transmitted power is −17 dBm and 0 dBm, respectively. In Fig. 10a, the following anchors have been set as a transmitter on the simulations: A00, A01, A03, A06, A09 and A11. In Fig. 10b, the following anchors have been set as a transmitter on the simulations: A12, A14, A16, A18, A20 and A22. These simulations have been configured to achieve a trade-off between the aforementioned recommendations trying to keep LoS conditions in the corridors and radio planning consideration based on the plant's characterization. In fact, depending on the percentage of efficiency the system's location can support, the number of anchors could be reduced since the cost for each of them is quite high. It is worth noting that it could be unnecessary to keep localization values less than 10cm for the load or forklifts tracking in T&W Logistics plant. The results show that the received power level is below the sensitivity requirement for both cases in the analyzed area (upper area in Fig. 10a and central area in Fig. 10b).

Fig. 11 shows the deployment of the UWB-based system in T&W Logistics plant. The deployment of the anchors has been performed at the heights of 2m, 3m and 4m on the racks. In order to ensure the quality of the links, and thus, high accuracy on the localization, more anchors have been

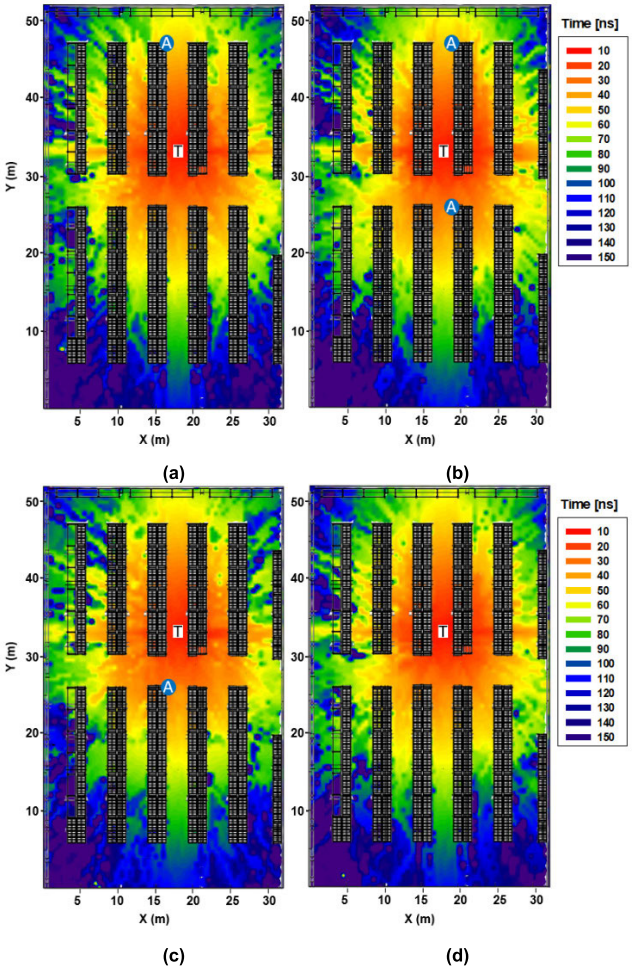

FIGURE 15. Estimated 2D ToF planes for test point 1 at the height of: (a) Anchor A08 (x = 16.74m; y = 47.26m; z = 3m); (b) Anchor A09 (x = 19.7m; y = 47.26; z = 2m) and anchor A20 (x = 19.7m; y = 26.27m; z = 2m); (c) Anchor A15 (x = 16.74m; y = 26.27; z = 4m); (d) Tag 038D (x = 18.3m, y = 33.1m, z = 2.4m).

deployed. Fig. 12 shows a capture of a real-time video of the tag tracking along corridor 4 (see Fig. 5a) using the open android app provided by DecaWave's development kit. After analyzing the results obtained by DecaWave devices for all the anchors deployed in T&W Logistics plant, it shows that in 90% of the plant, the estimated localization accuracy is less than 30cm. In the following subsection, the anchor's log information will be analyzed to compare with the 3D-RL time-domain estimations.

C. EVALUATION AND TIME-DOMAIN SIMULATIONS

In this subsection, the evaluation of the UWB-based localization system is presented. For this, a comparison of the ToF data provided by deployed DecaWave kits and estimations based on time-domain simulations using the 3D-RL tool are analyzed. As stated in Table 5, the DecaWave MDEK1001 development kit uses the DWM1001 module based on the radio transceiver IC DW1000 IEEE 802.15.4-2011 UWB. The DWM1001 operates in channel 5 (6.240-6.739 GHz), with 500 MHz bandwidth, preamble

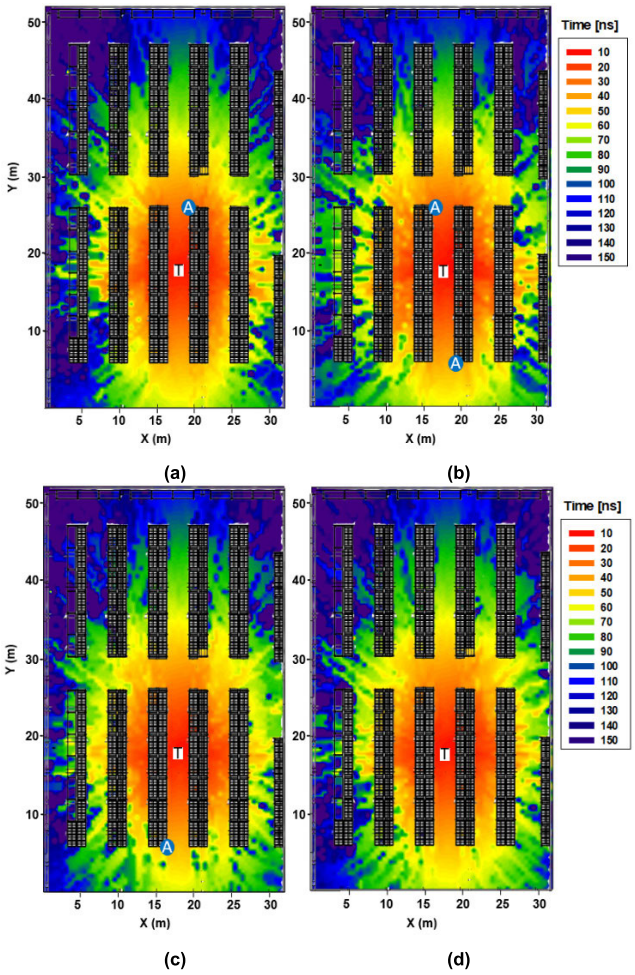

FIGURE 16. Estimated 2D ToF planes for test point 2 at the height of: (a) Anchor A20 (x = 19.7m; y = 26.27m; z = 2m); (b) Anchor A15 (x = 16.74m; y = 26.27; z = 4m and anchor A30 (x = 19.7m; y = 6.32; z = 4m); (c) Anchor A29 (x = 16.74m; y = 6.32m; z = 3m); (d) Tag 038D (x = 18.3m, y = 18.17 m, z = 2.4m).

length of 128, 64 MHz pulse repetition frequency and 6.8Mbps data rate. The localization algorithm is based on two-way ranging algorithm (TWR), that is, the ToF determination of the signal travelling in order to calculate the distance between two objects, as can be seen in Fig. 13 [42].

$$\text{Distance} = c \cdot ToF \tag{10}$$

As mentioned above, the ranging needs three-four anchors to carry out the trilateration algorithm to localize the tag (see Fig. 12). For the evaluation, several log files have been obtained of the tag position along corridor 4 (see Fig. 12a and 12b), with the anchors located in the same coordinates as Fig. 9. In these logs, information about the distance between the tag and each anchor is stored. Fig. 14 shows an example of samples gathered with an update rate of 10 Hz.

Table 6 and 7 present the localization distance error between the data provided by the DecaWave (DW) devices and the 3D-RL tool for test point 1 and test point 2,

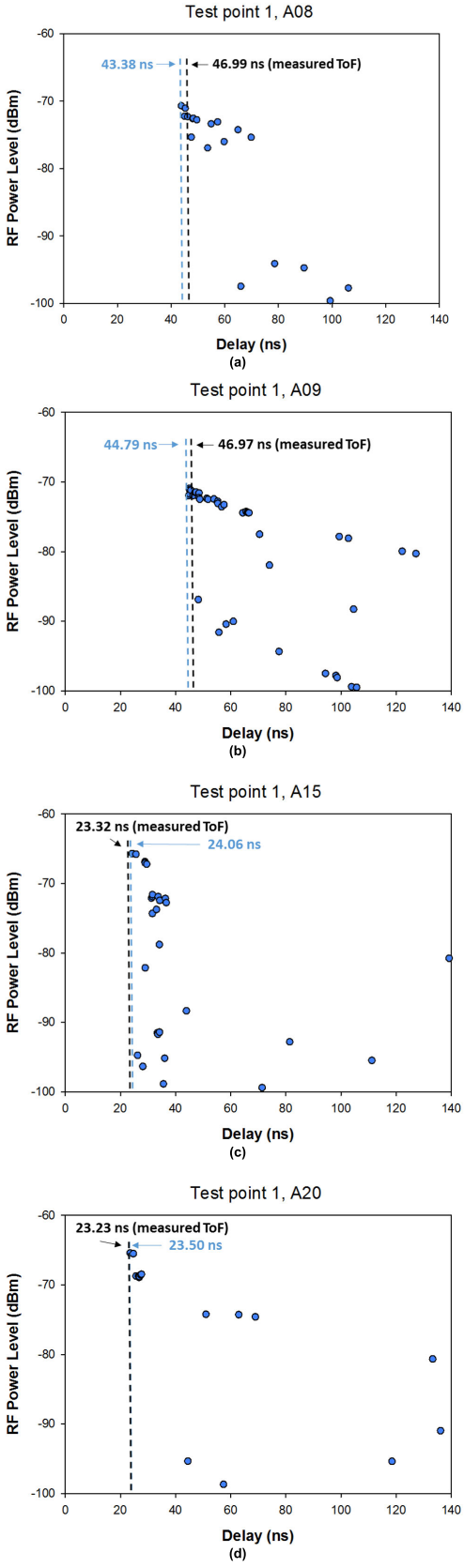

FIGURE 17. ToF results comparison between 3D RL estimations (PDP) and measurements corresponding to cases from Fig. 12 for Test point 1: (a) Anchor A08; (b) Anchor A09; (c) Anchor A15; (d) Anchor A20.

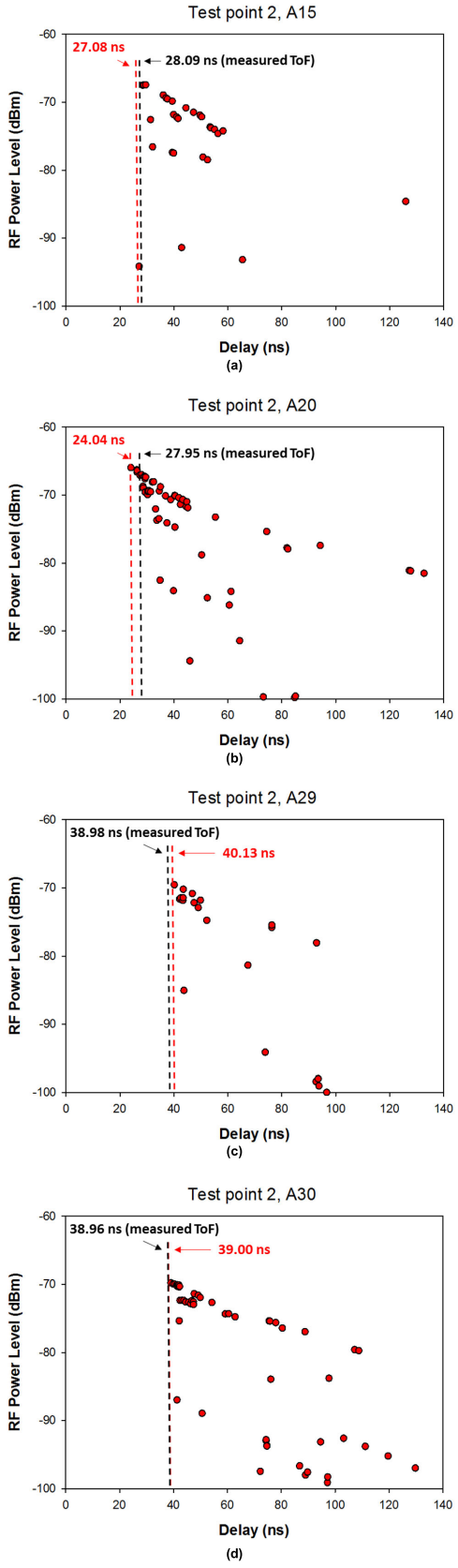

FIGURE 18. ToF results comparison between 3D RL estimations (PDP) and measurements corresponding to cases from Fig. 12 for test point 2: (a) Anchor A15; (b) Anchor A20; (c) Anchor A29; (d) Anchor A30.

respectively. With the distance from the log data and applying (2), ToF results have been obtained in order to compare with 3D-RL ToF estimations. Simulations have been launched according to the tag and anchors' real positions in Fig. 12, getting accurate results with respect to DecaWave devices, around sub-meter distance. The absolute error between measurements and simulations varies from 1cm to 120 cm, in the worst case, with an average error between all the results of 48.38cm. These estimated ranging variations provided by the ToF results of the 3D-RL tool are affected by the employed mesh resolution for the simulations, among other considerations, as explained in [14]. In this way, since the impinging rays are detected on the surface of the cuboids, the distance estimation varies depending on the cuboid location and the relative locations of Tx source and Rx observation point, leading to larger variations when the defined cuboid size is larger. Fig. 15 shows estimated 2D ToF planes in the time domain at the height of anchors A08, A09, A15 and A20 when the tag is located at test point 1. Fig. 16 shows estimated 2D ToF planes in the time domain at the height of anchors A15, A20, A29 and A30 when the tag is located at test point 2. Furthermore, Fig. 17 and Fig. 18 present the Power Delay Profiles (PDP) obtained by the 3D RL for both cases of Fig. 12 (Test Point 1 and Test Point 2), where the comparison between the estimated ToF (time to the first component of the PDP) and the measured ToF (vertical black dashed lines) is shown. As can be seen, the 3D-RL tool provides high accuracy estimations close to the DecaWave technology does, and therefore, the estimations could be used to optimize the deployment of the devices and keep the location requirements.

V. CONCLUSION

In this work, wireless channel characterization for UWB systems in industrial indoor logistic application has been described. A realistic logistic plant has been considered, in which volumetric characterization of the complete indoor scenario under analysis has been performed, with the aid of in-house hybrid deterministic 3D-RL approximation. Wireless channel analysis in frequency/power domain have been obtained for the 4 GHz and 6 GHz bands, validated by continuous wave (CW) measurement results, as well as by localization trials with anchors deployed within the scenario. The impact of object density is relevant in terms of resulting path loss as well as in time domain characterization, given by multipath propagation components, which has been described by considering different object density conditions. Time domain characterization results have been obtained and compared with measured time of flight results, showing good agreement and without the need of complex channel sounder system use. The proposed volumetric deterministic channel characterization can be applied in order to optimize node configuration and network topology, in order to maximize coverage whilst minimizing interference impact and energy consumption. As future work, a new firmware

will be developed in order to obtain parameters such as the Channel Impulse Response for a real-time localization within the logistic scenario of the vehicles (Forklifts and Automated Guided Vehicles), containers, pallets, tools, instrumentation or workers.

ACKNOWLEDGMENT

The authors would like to thank the Truck & Wheel Group for providing their facilities in Arazuri, Navarre (Spain) and overall support to carry out the deployment of the UWB kits, as well as to the OEE LOG project consortium.

REFERENCES

[1] S. Vitturi, C. Zunino, and T. Sauter, "Industrial communication systems and their future challenges: Next-generation Ethernet, IIoT, and 5G," *Proc. IEEE*, vol. 107, no. 6, pp. 944–961, Jun. 2019.

[2] E. Sisinni, A. Saifullah, S. Han, U. Jennehag, and M. Gidlund, "Industrial Internet of Things: Challenges, opportunities, and directions," *IEEE Trans. Ind. Informat.*, vol. 14, no. 11, pp. 4724–4734, Nov. 2018.

[3] C. M. D. Costa and P. Baltus, "Design methodology for industrial Internet-of-Things wireless systems," *IEEE Sensors J.*, vol. 21, no. 4, pp. 5529–5542, Feb. 2021, doi: 10.1109/JSEN.2020.3031659.

[4] L. Shu, M. Mukherjee, M. Pecht, N. Crespi, and S. N. Han, "Challenges and research issues of data management in IoT for large-scale petrochemical plants," *IEEE Syst. J.*, vol. 12, no. 3, pp. 2509–2523, Sep. 2018.

[5] J. Zhang, P. V. Orlik, Z. Sahinoglu, A. F. Molisch, and P. Kinney, "UWB systems for wireless sensor networks," *Proc. IEEE*, vol. 97, no. 2, pp. 313–331, Feb. 2009.

[6] P. Mayer, M. Magno, C. Schnetzler, and L. Benini, "EmbedUWB: Low power embedded high-precision and low latency UWB localization," in *Proc. IEEE 5th World Forum Internet Things (WF-IoT)*, Limerick, Ireland, Apr. 2019, pp. 519–523.

[7] G. Schroeer, "A real-time UWB multi-channel indoor positioning system for industrial scenarios," in *Proc. Int. Conf. Indoor Positioning Indoor Navigat. (IPIN)*, Nantes, France, Sep. 2018, pp. 1–5.

[8] A. R. J. Ruiz and F. S. Granja, "Comparing Ubisense, Bespoon, and Decawave UWB location systems: Indoor performance analysis," *IEEE Trans. Instrum. Meas.*, vol. 66, no. 8, pp. 2106–2117, Aug. 2017.

[9] C. Briso, C. Calvo, and Y. Xu, "UWB propagation measurements and modelling in large indoor environments," *IEEE Access*, vol. 7, pp. 41913–41920, 2019.

[10] A. Karaagac, J. Haxhibeqiri, M. Ridolfi, W. Joseph, I. Moerman, and J. Hoebeke, "Evaluation of accurate indoor localization systems in industrial environments," in *Proc. 22nd IEEE Int. Conf. Emerg. Technol. Factory Autom. (ETFA)*, Limassol, Cyprus, Sep. 2017, pp. 1–8.

[11] V. Barral, P. Suárez-Casal, C. J. Escudero, and J. A. García-Naya, "Multi-sensor accurate forklift location and tracking simulation in industrial indoor environments," *Electronics*, vol. 8, no. 10, p. 1152, Oct. 2019.

[12] F. Holzke, P. Danielis, F. Golatowski, and D. Timmermann, "A fusion approach for the localization of humans in factory environments," in *Proc. IEEE Ind. Cyber-Phys. Syst. (ICPS)*, St. Petersburg, Russia, May 2018, pp. 59–64.

[13] M. Ridolfi, S. Van de Velde, H. Steendam, and E. De Poorter, "Analysis of the scalability of UWB indoor localization solutions for high user densities," *Sensors*, vol. 18, no. 6, p. 1875, 2018.

[14] T. Otim, P. Lopez-Iturri, L. Azpilicueta, A. Bahillo, L. E. Diez, and F. Falcone, "A 3D ray launching time-frequency channel modeling approach for UWB ranging applications," *IEEE Access*, vol. 8, pp. 97321–97334, 2020.

[15] T. Otim, A. Bahillo, L. E. Diez, P. Lopez-Iturri, and F. Falcone, "Impact of body wearable sensor positions on UWB ranging," *IEEE Sensors J.*, vol. 19, no. 23, pp. 11449–11457, Dec. 2019, doi: 10.1109/JSEN.2019.2935634.

[16] T. Otim, A. Bahillo, L. E. Díez, P. Lopez-Iturri, and F. Falcone, "Towards sub-meter level UWB indoor localization using body wearable sensors," *IEEE Access*, vol. 8, pp. 178886–178899, 2020.

[17] *Truck & Wheel Group*. Accessed: Mar. 22, 2021. [Online]. Available: https://tw-group.com/en/

[18] R. Candell, M. Kashef, Y. Liu, K. B. Lee, and S. Foufou, "Industrial wireless systems guidelines: Practical considerations and deployment life cycle," *IEEE Ind. Electron. Mag.*, vol. 12, no. 4, pp. 6–17, Dec. 2018.

[19] Y. Liu, M. Kashef, K. B. Lee, L. Benmohamed, and R. Candell, "Wireless network design for emerging IIoT applications: Reference framework and use cases," *Proc. IEEE*, vol. 107, no. 6, pp. 1166–1192, Jun. 2019.

[20] X. Jiang, Z. Pang, M. Luvisotto, R. Candell, D. Dzung, and C. Fischione, "Delay optimization for industrial wireless control systems based on channel characterization," *IEEE Trans. Ind. Informat.*, vol. 16, no. 9, pp. 5855–5865, Sep. 2020.

[21] J. Narrainen and R. D'Errico, "Large scale channel parameters in industrial environment," in *Proc. 13th Eur. Conf. Antennas Propag. (EuCAP)*, Krakow, Poland, Mar. 2019, pp. 1–5.

[22] D. Block, N. H. Fliedner, D. Toews, and U. Meier, "Wireless channel measurement data sets for reproducible performance evaluation in industrial environments," in *Proc. IEEE 20th Conf. Emerg. Technol. Factory Autom. (ETFA)*, Luxembourg, U.K., Sep. 2015, pp. 1–4.

[23] M. Razzaghpour, R. Adeogun, I. Rodriguez, G. Berardinelli, R. S. Mogensen, T. Pedersen, P. Mogensen, and T. B. Sorensen, "Short-range UWB wireless channel measurement in industrial environments," in *Proc. Int. Conf. Wireless Mobile Comput., Netw. Commun. (WiMob)*, Barcelona, Spain, Oct. 2019, pp. 1–6.

[24] M. Cheffena, "Propagation channel characteristics of industrial wireless sensor networks [wireless corner]," *IEEE Antennas Propag. Mag.*, vol. 58, no. 1, pp. 66–73, Feb. 2016, doi: 10.1109/MAP.2015.2501227.

[25] J. Karedal, S. Wyne, P. Almers, F. Tufvesson, and A. F. Molisch, "A measurement-based statistical model for industrial ultra-wideband channels," *IEEE Trans. Wireless Commun.*, vol. 6, no. 8, pp. 3028–3037, Aug. 2007.

[26] R. J. Luebbers, "A heuristic UTD slope diffraction coefficient for rough lossy wedges," *IEEE Trans. Antennas Propag.*, vol. 37, no. 2, pp. 206–211, Feb. 1989.

[27] R. J. Luebbers, "Comparison of lossy wedge diffraction coefficients with application to mixed path propagation loss prediction," *IEEE Trans. Antennas Propag.*, vol. 36, no. 7, pp. 1031–1034, Jul. 1988.

[28] L. Azpilicueta, M. Rawat, K. Rawat, F. Ghannouchi, and F. Falcone, "Convergence analysis in deterministic 3D ray launching radio channel estimation in complex environments," *Appl. Comput. Electromagn. Soc. J.*, vol. 29, no. 4, pp. 256–271, 2014.

[29] L. Azpilicueta, F. Falcone, and R. Janaswamy, "Hybrid computational techniques: Electromagnetic propagation analysis in complex indoor environments," *IEEE Antennas Propag. Mag.*, vol. 61, no. 6, pp. 20–30, Dec. 2019, doi: 10.1109/MAP.2019.2943297.

[30] L. Azpilicueta, E. Aguirre, P. López-Iturri, and F. Falcone, "An accurate UTD extension to a ray-launching algorithm for the analysis of complex indoor radio environments," *J. Electromagn. Waves Appl.*, vol. 30, no. 1, pp. 43–60, Jan. 2016.

[31] L. Azpilicueta, M. Rawat, K. Rawat, F. Ghannouchi, and F. Falcone, "A ray launching-neural network approach for radio wave propagation analysis in complex indoor environments," *IEEE Trans. Antennas Propag.*, vol. 62, no. 5, pp. 2777–2786, May 2014.

[32] F. A. Rodríguez-Corbo, L. Azpilicueta, M. Celaya-Echarri, P. Lopez-Iturri, I. Picallo, F. Falcone, and A. V. Alejos, "Deterministic 3D ray-launching millimeter wave channel characterization for vehicular communications in urban environments," *Sensors*, vol. 20, no. 18, p. 5284, Sep. 2020.

[33] V. Komarov, *Handbook on Dielectric & Thermal Properties of Materials at Microwave Frequencies*. Norwood, MA, USA: Artech House, 2012.

[34] *Effects of Building Materials and Structures on Radiowave Propagation Above About 100 MHz*. Accessed: Jul. 6, 2021. [Online]. Available: https://www.itu.int/rec/R-REC-P.2040-1-201507-I/en

[35] L. Azpilicueta, P. López-Iturri, E. Aguirre, C. Vargas-Rosales, A. León, and F. Falcone, "Influence of meshing adaption in convergence performance of deterministic ray launching estimation in indoor scenarios," *J. Electromagn. Waves Appl.*, vol. 31, no. 5, pp. 544–559, 2017.

[36] A. F. Molisch, K. Balakrishnan, C.-C. Chong, S. Emami, A. Fort, J. Karedal, J. Kunisch, H. Schantz, U. Schuster, and K. Siwiak, *IEEE 802.15.4a Channel Model-Final Report*, Standard P802 154 0662, 2004.

[37] J. Karedal, S. Wyne, P. Almers, F. Tufvesson, and A. F. Molisch, "Statistical analysis of the UWB channel in an industrial environment," in *Proc. IEEE 60th Veh. Technol. Conf.*, Los Angeles, CA, USA, Sep. 2004, pp. 81–85.
[38] C. Suwatthikul, W. Chantaweesomboon, S. Manatrinon, K. Athikulwongse, and K. Kaemarungsi, "Implication of anchor placement on performance of UWB real-time locating system," in *Proc. 8th Int. Conf. Inf. Commun. Technol. Embedded Syst. (IC-ICTES)*, Chonburi, Thailand, May 2017, pp. 1–6.
[39] R. Simedroni, E. Puschita, T. Palade, P. Dolea, C. Codau, R. Buta, and A. Pastrav, "Indoor positioning using Decawave MDEK1001," in *Proc. Int. Workshop Antenna Technol. (iWAT)*, Bucharest, Romania, Feb. 2020, pp. 1–4.
[40] A. Pastrav, R. Simedroni, T. Palade, P. Dolea, D. Popescu, and E. Puschita, "Evaluation of UWB transmissions in highly reflective environments," in *Proc. 13th Int. Conf. Commun. (COMM)*, Bucharest, Romania, Jun. 2020, pp. 527–532.
[41] *Decawave*. Accessed: Mar. 23, 2021. [Online]. Available: https://www.decawave.com/
[42] *APS013 Application Note*. Accessed: May 13, 2021. [Online]. Available: https://www.decawave.com/application-notes/

IMANOL PICALLO GUEMBE received the bachelor's degree in telecommunications engineering from the Public University of Navarre (UPNA), in 2016, and the master's degree in telecommunication engineering from Charles III University of Madrid (UC3M), in 2019. He is currently pursuing the Ph.D. degree in communication engineering with UPNA. He worked as a Developer at Zener Group Company and is currently working on several public and privately funded research projects. He has over ten contributions in indexed international journals and conference contributions. His research interests include radio propagation in inhomogeneous environments, human–body interference analysis, wireless sensor networks, the IoT networks, and 5G communications systems. He has been awarded the ISSI 2019 Best Paper Award.

PEIO LOPEZ-ITURRI received the degree in telecommunications engineering, the master's degree in communications, and the Ph.D. degree in communication engineering from the Public University of Navarre (UPNA), Pamplona, Navarre, in 2011, 2012, and 2017, respectively. He has worked in ten different public and privately funded research projects. In 2019, he partly worked as a Researcher at Tafco Metawireless. He is currently affiliated with the Institute for Smart Cities (ISC), UPNA. He gets the 2018 Best Spanish Ph.D. Thesis in Smart Cities in CAEPIA 2018 (3rd prize), sponsored by the Spanish Network on Research for Smart Cities CI-RTI and Sensors (ISSN 1424-8220). He has over 150 contributions in indexed international journals, book chapters, and conference contributions. His research interests include radio propagation, wireless sensor networks, electromagnetic dosimetry, modeling of radio interference sources, mobile radio systems, wireless power transfer, the IoT networks and devices, 5G communication systems, and EMI/EMC. He has been awarded the ECSA 2014 Best Paper Award, the IISA 2015 Best Paper Award, and the ISSI 2019 Best Paper Award.

HICHAM KLAINA received the master's degree in networks and telecommunications engineering from the National School of Applied Sciences of Tetouan (ENSATé), Morocco, in 2016. He is currently pursuing the Ph.D. degree in telecommunications engineering with the University of Vigo, Spain. He has over ten contributions in indexed international journals and conference contributions. His research interests include smart agriculture, near-ground radio propagation, wireless sensor networks, vehicular communication, channel modeling, the IoT networks and devices, RFID, and 5G communication systems. He has been awarded the Best Final Year Project Award by the National School of Applied Sciences of Tetouan, in 2016, the 2017 Predoctoral Research Grant supported by the Xunta de Galicia, and the ECSA-4 Best Paper Award, in 2017.

GUILLERMO GLARIA EZKER received the master's degree in telecommunications engineering from the Public University of Navarre (UPNA), Pamplona, Navarre, in 2000. He has worked in more than 50 different public and privately funded research projects. In 2000, he joined NAITEC—Technological Center for Automotive and Mechatronics as a Researcher of the Mechatronics Business Unit. His research interests include embedded software programming, the IoT systems, wireless sensor network protocols, heterogeneous sensors, ultra-low power devices, and real-time location systems.

FÉLIX SÁEZ DE JAUREGUI URDANOZ received the master's degree in telecommunications engineering from the Public University of Navarre (UPNA), Pamplona, Navarre, in 1999. He has worked in more than 50 different public and privately funded research projects. In 2000, he joined NAITEC—Technological Center for Automotive and Mechatronics as a Researcher of the Mechatronics Business Unit. His research interests include embedded software programming, the IoT systems, wireless sensor networks, and real-time location systems.

JOSÉ LUIS ZABALZA CESTAU received the master's degree in telecommunications engineering from Ramon Llull University (URL), Barcelona, Catalunya, in 1993. He has worked in more than 50 different public and privately funded research projects. In 2001, he joined NAITEC—Technological Center for Automotive and Mechatronics as a Researcher of the Mobility Business Unit. His research interests include embedded linux software programming, sensors interfaces, protocol and communication buses, and real time operating systems.

LEYRE AZPILICUETA (Senior Member, IEEE) received the degree in telecommunications engineering, the master's degree in communications, and the Ph.D. degree in telecommunication technologies from the Public University of Navarre (UPNA), Spain, in 2009, 2011, and 2015, respectively. In 2010, she worked as a Radio Engineer with Research and Development Department, RFID Osés. She is currently working as an Associate Professor and a Researcher at the Tecnologico de Monterrey, Campus Monterrey, Mexico. She has over 200 contributions in relevant journals and conference publications. Her research interests include radio propagation, mobile radio systems, wireless sensor networks, ray tracing, and channel modeling. She has been a recipient of the 'IEEE Antennas and Propagation Society Doctoral Research Award 2014,' the 'Young Professors and Researchers Santander Universities 2014 Mobility Award,' the ECSA 2014 Best Paper Award, the IISA 2015 Best Paper Award, the Best Ph.D. Award by the Colegio Oficial de Ingenieros de Telecomunicación, in 2016, the 'N2Women: Rising Stars in Computer Networking and Communications' 2018 Award, the ISSI 2019 Best Paper Award, and the Junior Research Raj Mittra Travel Grant 2020.

FRANCISCO FALCONE (Senior Member, IEEE) received the degree in telecommunication engineering and the Ph.D. degree in communication engineering from the Universidad Pública de Navarra (UPNA), Spain, in 1999 and 2005, respectively. From February 1999 to April 2000, he was a Microwave Commissioning Engineer with SiemensItaltel, deploying microwave access systems. From May 2000 to December 2008, he was a Radio Access Engineer with Telefónica Móviles, performing radio network planning and optimization tasks in mobile network deployment. He was an Assistant Lecturer with the Electrical and Electronic Engineering Department, UPNA, from February 2003 to May 2009. From January 2009 to May 2009, he was a Co-Founding Member and the Director of Tafco Metawireless, a spin-off company from UPNA. In June 2009, he become an Associate Professor with the EE Department, being the Department Head, from January 2012 to July 2018, and since July 2019. From January 2018 to May 2018, he was a Visiting Professor with Kuwait College of Science and Technology, Kuwait. He is also affiliated with the Institute for Smart Cities (ISC), UPNA, which hosts around 140 researchers and currently acting as the Head of ISC. His research interests include computational electromagnetics applied to analysis of complex electromagnetic scenarios, with a focus on the analysis, design, and implementation of heterogeneous wireless networks to enable context aware environments. He has more than 500 contributions in indexed international journals, book chapters, and conference contributions. He received the CST 2003 and CST 2005 Best Paper Award, the Ph.D. Award from the Colegio Oficial de Ingenieros de Telecomunicación (COIT), in 2006, the Doctoral Award UPNA, in 2010, the 1st Juan Gomez Peñalver Research Award from the Royal Academy of Engineering of Spain, in 2010, the XII Talgo Innovation Award 2012, the IEEE 2014 Best Paper Award, in 2014, the ECSA-3 Best Paper Award, in 2016, and the ECSA-4 Best Paper Award, in 2017.